Geophysical Research Letters

Key Points:
- Cloud longwave scattering is more important in the polar regions than the extrapolar regions
- By surface-atmosphere radiative coupling, cloud longwave scattering can warm the polar surface, more in the winter than in the summer
- Cloud longwave scattering is a necessity instead of an option for correctly simulating polar climate and surface energy budget

Supporting Information:
- Supporting Information S1

Correspondence to:
Y.-H. Chen,
yihsuan@umich.edu

Seasonal Dependent Impact of Ice Cloud Longwave Scattering on the Polar Climate

Yi-Hsuan Chen[1,2] (iD), **Xianglei Huang**[1] (iD), **Ping Yang**[3], **Chia-Pang Kuo**[3,4] (iD), and **Xiuhong Chen**[1] (iD)

[1]Department of Climate and Space Sciences and Engineering, University of Michigan, Ann Arbor, MI, USA, [2]Now at Program in Atmospheric and Oceanic Sciences, Princeton University, Princeton, NJ, USA, [3]Department of Atmospheric Sciences, Texas A&M University, College Station, TX, USA, [4]Now at Department of Atmospheric Sciences, Colorado State University, Fort Collins, CO, USA

Abstract Most climate models neglect cloud longwave (LW) scattering because scattering is considered negligible compared to strong LW absorption by clouds and greenhouse gases. While this rationale is valid for simulating extrapolar regions, it is questionable for the polar regions, where the atmosphere is dry and hence has weak absorption, and ice clouds that have strong scattering capability frequently occur. Using the slab-ocean Community Earth System Model, we show that ice cloud LW scattering can warm winter surface air temperature by 0.8–1.8 K in the Arctic and 1.3–1.9 K in the Antarctic, while this warming becomes much weaker in polar summer. Such scattering effect cannot be correctly assessed when sea surface temperature and sea ice are prescribed as this effect is manifested through a surface-atmosphere coupling. Cloud LW scattering is a necessity for the correct simulation of polar climate and surface radiation budget, especially in the winter.

Plain Language Summary Cloud longwave scattering has never been deemed as a necessity in climate models. Out of all climate models in the IPCC fifth and sixth assessments, only three modeling centers have longwave scattering included in their models. Our study explained why the traditional wisdom of neglecting longwave scattering breaks down for the simulation of high-latitude climate in the fully coupled models. We showed the critical importance of atmosphere-surface radiative coupling for correctly assessing the role of cloud longwave scattering in the model simulation of climate mean state as well as climate changes, an issue overlooked by all previous studies. We argued that the cloud longwave scattering is a necessity in climate models, not an option.

1. Introduction

Cloud-radiation interactions play an important role in the Earth's climate system (Stephens, 2005, and references therein), and sustained efforts have been invested in cloud-radiation parameterizations in climate models (Edwards & Slingo, 1996; Fu & Liou, 1993; Mlawer et al., 1997; Pincus et al., 2003; Randall, 1989; Stephens, 1984; Yang et al., 2015). A cloud can absorb and scatter incident radiation and emit longwave (LW) radiation itself. Accurately modeling radiative transfer in a scattering atmosphere is computationally infeasible for climate model simulations, so reasonable approximations and simplifications have to be made. One widely used approximation is the neglect of cloud LW scattering (supporting information Text S1). The traditional justification for this approximation is twofold: (1) the imaginary parts of the index of refraction of both ice and liquid in the LW are orders of magnitude larger than the counterparts in the shortwave. Therefore, the overall attenuation of LW radiation by clouds is largely caused by absorption rather than scattering. (2) Furthermore, the LW has strong gaseous absorption by H_2O, CO_2, O_3, and other trace gases. The single-scattering albedo of a vertical layer in the atmosphere, which describes the probability that an attenuated photon is scattered instead of being absorbed in the layer, can be expressed as

$$\omega = \frac{\omega_c \tau_c}{\tau_{air} + \tau_c},$$
(1)

where τ_{air} and τ_c are the extinction optical thickness of gases and cloud in the layer, respectively, and ω_c is the single-scattering albedo of cloud. Note that all variables in Equation 1 are frequency dependent. As long as $\tau_{air} \gg \tau_c$, the scattering in the layer is negligible regardless of the value of ω_c.

In the tropics and midlatitudes, water vapor is abundant, so $\tau_{air} \gg \tau_c$ in the water vapor bands, implying negligible scattering in these bands. This condition, however, breaks down in polar regions for three reasons. First, the imaginary part of the index of refraction of ice has a local minimum around 400 cm^{-1}; as a result, ice clouds can have a single-scattering albedo as large as 0.6–0.8 over 350–630 cm^{-1}, a portion of the far-IR (10–650 cm^{-1}) spectrum (supporting information Figure S1). Second, the same portion of the far-IR spectrum, where ice clouds exhibit strong scattering, contributes ~35–40% of outgoing LW radiation (OLR) (supporting information Figure S2b) and ~50–65% of downward LW radiation in the polar regions; thus, its contribution to energy budgets is not small. Third, the high-latitude total column water vapor (TCWV) is much smaller than the TCWV in extrapolar regions (supporting information Figure S2a). The TCWV in the deep Antarctic is often <2 mm owing to its high elevation, and the winter to summer TCWV varies by a factor of ~2.5; in the Arctic, the TCWV is slightly above 10 mm only in the summer and the summer-to-winter variation can be a factor of 4–5. Since the optical depth is proportional to the column density of the absorber, the optical depth of water vapor in high latitudes is also significantly less than those in the extrapolar regions. Therefore, even for the same ice cloud, the scattering effect for the entire atmospheric layer can be larger in the high latitudes than in the rest of the globe simply because τ_{air} caused by water vapor absorption is small in the polar regions. Such scattering effects can be especially important over the aforementioned far-IR region where ice scattering effects peak and contribute to a large portion of the LW radiation budget.

In this study, we investigate the ice cloud LW scattering effect on the simulated climate using a modified version of Community Earth System Model (CESM) version 1.1.1. The scattering effects of liquid clouds are generally small over the entire LW (supporting information Figure S1) and are not included in this study. A number of studies have investigated the influence of cloud LW scattering using climate model simulations (Jin et al., 2019; Wu et al., 2019; Zhao et al., 2018). Interestingly, none of these studies report the influences of cloud LW scattering in the polar regions. We speculate that because all these studies carried out climate simulations with prescribed sea surface temperatures (SSTs) and sea ice concentration, the LW radiative boundary condition is hence prescribed over oceans, thus limiting the surface response to the changes in LW flux due to cloud LW scattering. This study will reveal the role of atmosphere-surface coupling in assessing the cloud LW scattering effect in polar regions.

2. Methods

2.1. The Modified Version of CESM 1.1.1

The CESM 1.1.1 slab-ocean model (SOM) configuration (Hurrell et al., 2013) is used in this study, with default CAM4 physics package (Neale et al., 2010) except the radiation schemes, which have been manually configured to RRTMG_LW and RRTMG_SW, that is, the schemes used in CAM5 (Neale et al., 2012). Because the model does not parameterize the LW scattering properties of clouds (Mitchell et al., 1996) nor its LW radiation scheme (RRTMG_LW; Mlawer et al., 1997) takes LW scattering into account, a new ice cloud-radiation scheme and a modified version of the RRTMG_LW are implemented into the model. This new ice cloud LW radiation scheme is developed by Kuo et al. (2020), which parameterizes ice cloud extinction coefficient, single-scattering albedo, and the asymmetry factor based on the MODIS (Moderate Resolution Imaging Spectroradiometer) Collection 6 ice cloud model (Platnick et al., 2017) with in situ observed particle size distributions (Baum et al., 2011; Heymsfield et al., 2010, 2013). These obtained ice cloud LW optical properties were regressed as a function of the cloud ice particle effective diameter. The cloud ice effective diameter is parameterized as a function of temperature based on Kristjánsson et al. (2000), which is part of the CAM4 default cloud microphysics scheme.

The modified version of the RRTMG_LW scheme used in this study is also described in Kuo et al. (2020). This scheme uses a hybrid two-stream and four-stream (2S/4S) radiative transfer solver (Fu et al., 1997; Toon et al., 1989) to handle LW scattering calculations. Compared to the 128-stream DISORT solver (DIScrete Ordinate Radiative Transfer; Stamnes et al., 1988), this modified RRTMG_LW scheme is accurate enough and computationally efficient in both clear and cloudy conditions (Kuo et al., 2020).

It would be instructive to show the ice cloud LW scattering effects from offline radiative transfer calculations, using the modified RRTMG_LW schemes described above with a typical sub-Arctic summer profile (McClatchey et al., 1972). In these offline calculations, a layer of ice cloud with depth of 1 km is put at 7–
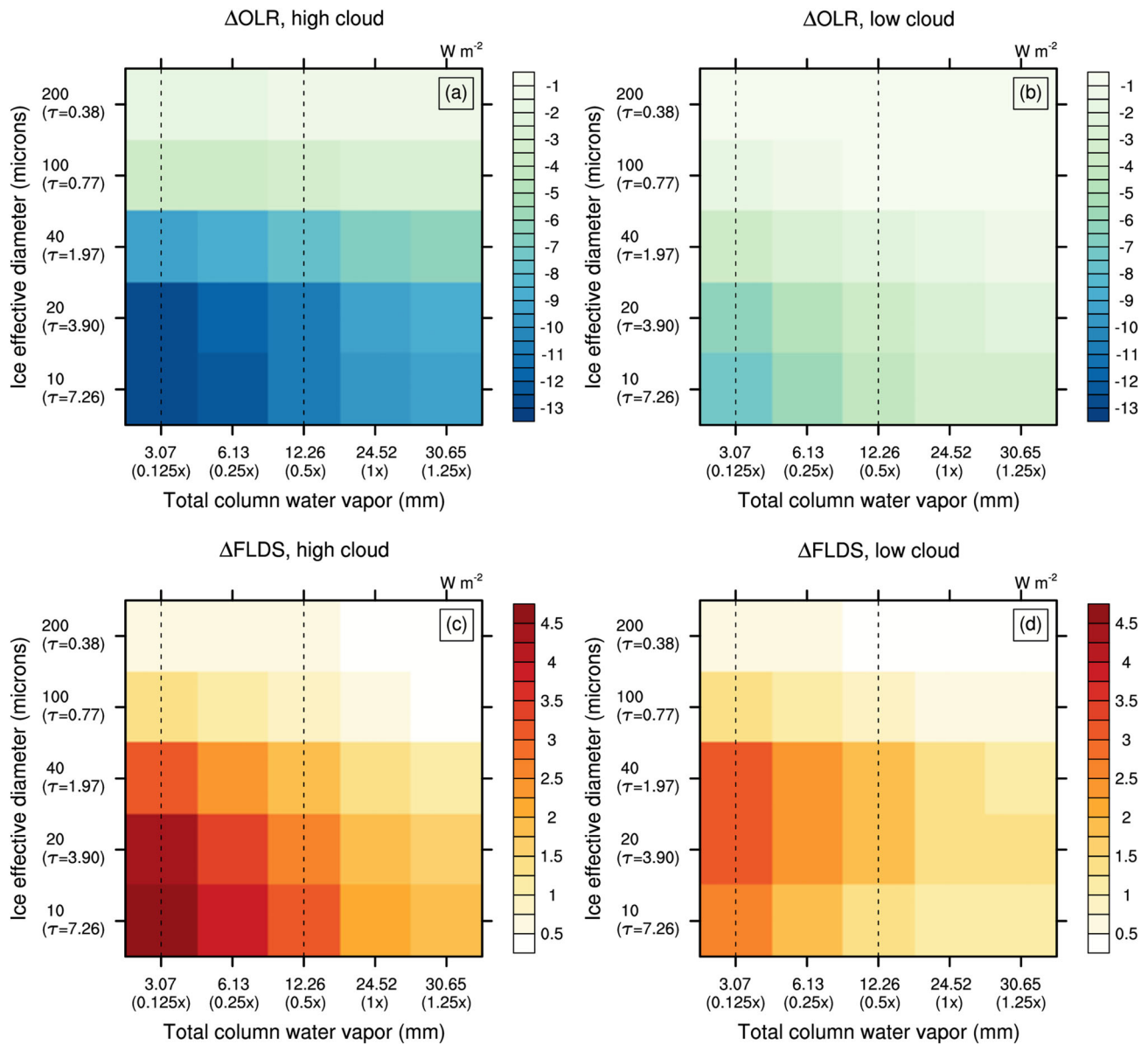
Figure 1. (a, b) Off-line radiative transfer calculation of the change of OLR (ΔOLR) due to the inclusion of ice cloud longwave scattering for different combinations of TCWV and ice cloud effective diameter. The optical depth in the infrared window (909 cm^{-1}) is indicated on Y axis. Left panel is for the case of high-cloud and right for the low-cloud case. (c, d) Same as (a) and (b), respectively, except for change of FLDS (ΔFLDS). On each panel, two vertical dashed lines denote the typical TCWV for Arctic winter (left) and summer (right), respectively.

8 km as a high-cloud case or at 1–2 km as a low-cloud case. The ice water path is fixed to 50 gm^{-2}, which is a typical value for polar clouds. To represent different cloud optical depth, the ice particle effective diameter is varied from 10 to 200 μm. To show the dependence on the TCWV, the aforementioned sub-Arctic summer humidity profile is scaled by a factor from 0.125 to 1.25 to cover the range of TCWV from polar summer to winter. The ice cloud LW scattering effect on OLR and downward LW flux at the surface (FLDS) is shown in Figure 1.

Consistent with previous studies (Costa & Shine, 2006; Kuo et al., 2017), inclusion of LW scattering leads to reduction of OLR and increase of FLDS. The scattering effect of low clouds is generally smaller than for high clouds, which can be explained using Equation 1, because τ_{air} due to water vapor absorption in the lower troposphere is much larger than in the upper troposphere. Like the case of shortwave, for the same ice water path, smaller cloud ice particles result in stronger scattering effect. When the ambient water vapor
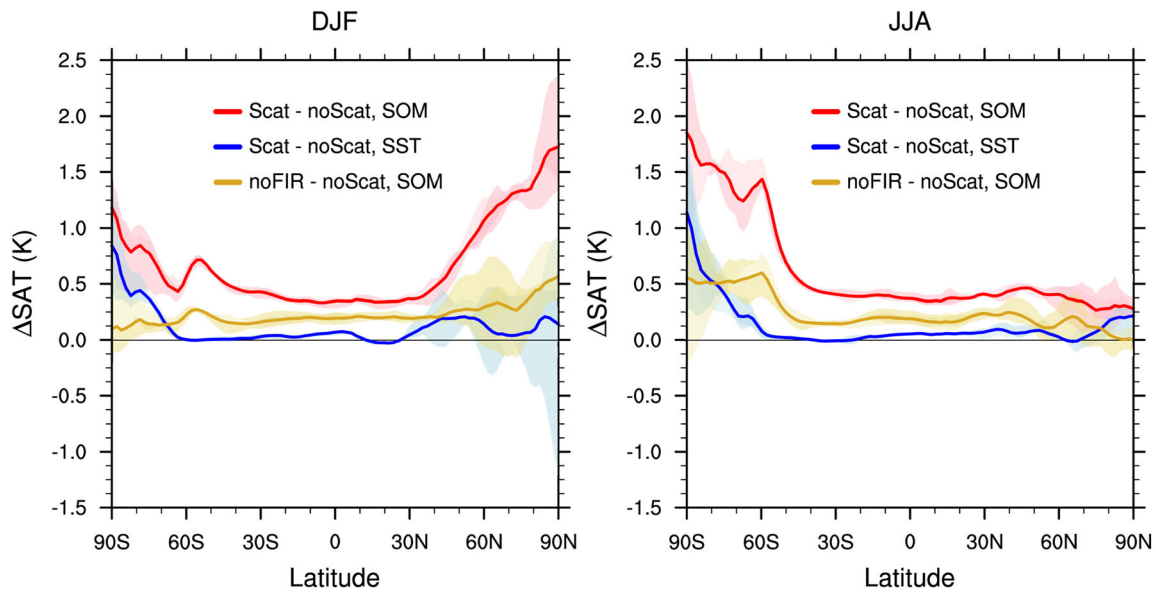
Figure 2. Left panel: Changes of DJF, zonal-mean surface air temperature (ΔSAT) due to inclusion of ice cloud LW scattering in the CESM. Each solid line shows an ensemble-mean difference and shading shows the spread of four 30-year ensemble runs. Red indicates the difference between Scat and noScat in the SOM simulations. Blue shows the same difference from the prescribed SST simulations. Yellow is the same as red but for the difference between noFIR and noScat. Right panel: Same as left panel but for JJA.

increases (i.e., large TCWV), the scattering effect is reduced, which again can be explained using Equation 1. These features above suggest that, compared to moist tropics and midlatitudes, cloud LW scattering likely plays a more important role in the dry polar regions, as the polar region has smaller TCWV and ice clouds frequently occur throughout the year. In addition, given that the TCWV in polar regions varies substantially between winter and summer (supporting information Figure S2a), the scattering effect can be stronger in polar winter than summer.

2.2. CESM Simulation Settings

Using the modified version of CESM1.1.1, three sets of experiments are carried out. The first set of experiments enables the ice cloud LW scattering effect (hereby referred to as "Scat"). The second set is the same, except cloud LW scattering is turned off by setting the cloud extinction optical depth to the absorption optical depth and the cloud single scattering albedo to zero ("noScat"). To examine the contributions from the far-IR bands, the third set is also the same as Scat, except the ice cloud scattering in the far-IR bands is turned off ("noFIR"). The impact of ice cloud LW scattering on the simulated climate is then deduced by differencing the results from Scat and noScat runs or from noFIR and noScat runs. To understand how ice cloud LW scattering interacts with surface energy processes, these three experiments were carried out with a SOM, where SST and sea ice can have thermodynamic responses to the change of surface energy. We also carried out the same three sets of experiments with prescribed climatological SST and sea ice concentration. All simulations are forced with recent forcings at the level of year 2000. Four 35-year ensemble runs were performed in each experiment to account for model internal variability. The last 30 years of simulations is analyzed. The horizontal resolution of the simulations is 1.9^{o} latitude by 2.5^{o} longitude. Additional details about the simulation settings can be found in the supporting information Text S2.

3. Result Discussions

3.1. The Ice Cloud LW Scattering Effect on Surface Air Temperature

Now we start to examine the impacts of ice cloud LW scattering on the simulated climate. Figure 2 shows the impacts on the simulated zonal-mean surface air temperature (SAT) climatology for December-January-February (DJF) and June-July-August (JJA) periods, respectively. For prescribed SST runs, including or excluding LW scattering has little impact on simulated SAT except in the Antarctic region.

This is consistent with traditional wisdom that LW scattering matters little in prescribed SST simulations. The simulated SAT difference (ΔSAT) south of 60°S is explainable because the Antarctic continent covers a majority of the region and the land surface temperature can respond to the changes due to the ice cloud LW scattering. Over the Arctic, the ensemble-mean ΔSAT is nearly zero but the ΔSAT of an individual member can be either positive or negative. This indicates that, when SST and sea ice are prescribed, including or excluding LW scattering behaves as a noisy perturbation on top of the already large internal variability of Arctic climate, and the ensemble-mean difference in SAT is not statistically different from zero.

However, the zonal-mean SAT difference due to ice cloud LW scattering for the SOM runs is positive everywhere in all ensemble members (Figure 2). Ensemble spreads in SOM runs are well separated from their counterparts in the prescribed SST runs. The ensemble-mean ΔSAT in the extrapolar regions is ~0.5 K for both DJF and JJA periods. In contrast, the Arctic ensemble-mean ΔSAT is ~1.8 K in DJF and ~0.4 K in JJA, that is, an ~4 time differences between the summer and winter seasons. Moreover, all ensemble members show consistently positive ΔSAT increases in the Arctic in spite of the large internal variability. Two factors explain the large contrast between the Arctic summer and winter ΔSAT: (1) the seasonality of Arctic TCWV as mentioned above (less winter TCWV implies a stronger LW scattering effect) and (2) the absence of shortwave radiation and reduced surface turbulent heat flux due to extensive ice coverage in winter lead to a radiative boundary layer with LW radiation playing a dominant role in regulating SAT (Overland & Guest, 1991; Serreze & Barry, 2005). In contrast, solar radiation plays a leading role in the summer Arctic surface energy balance. The ensemble-mean, Arctic domain-averaged net solar radiation at surface is 97.5 W m^{-2}, much larger than the net LW radiation (32.2 W m^{-2}), sensible heat flux (8.4 W m^{-2}), and latent heat flux (14.2 W m^{-2}) (supporting information Figure S7). Moreover, summer snow and ice melting consumes energy and reduces energy available to further warm the surface. Similar contrasts between winter and summer ΔSAT can be seen in the Antarctic.

Yellow curves in Figure 2 show the impact on zonal-mean SAT when ice cloud scattering is turned off in the far-IR but on in the mid-IR (i.e., noFIR-noScat). Here mid-IR refers to the spectral region between 650 and 2,500 cm^{-1}. Mid-IR scattering contributes to about half of total ΔSAT in the extrapolar regions. The mid-IR scattering primarily results from window regions (800–1,200 cm^{-1}), where gaseous absorption is weak and thus τ_{air} is small. However, for both Arctic and Antarctic winter, ΔSAT in the noFIR run is much smaller than in the Scat run, indicating the dominant contribution of far-IR scattering to ΔSAT in the Scat run. Such a contrasting role of ice cloud far-IR scattering between polar winter and extrapolar regions can be largely understood using Equation 1 and is primarily due to the drastic winter difference in TCWV (and hence $\Delta\tau_{air}$) between extrapolar and polar regions. It is also partly due to the increasing importance of far-IR contributions to the LW radiation from tropics to polar regions (supporting information Figure S2b).

3.2. Ice Cloud LW Scattering Manifested by Surface-Atmosphere LW Radiative Coupling

Figure 3 includes several key diagnostics to reveal the reasons behind the differences between the SOM and prescribed SST runs. For both runs, the Arctic winter domain-averaged ΔSAT is well correlated with the difference in FLDS (ΔFLDS) caused by the ice cloud LW scattering. A linear regression can explain >90% of the variance in ΔSAT, and the linear regression slope is essentially the same for both the SOM and prescribed SST runs (Figure 3a). The linear relations still hold for Arctic summer but can only explain ~55% of the variance. (Figure 3c). These are consistent with the dominant role of LW radiation in regulating wintertime SAT. Similar good linear relations can also be found between wintertime ΔFLDS and ΔTCWV (Figure 3b) and between zonal-mean ΔSAT and ΔFLDS as well as zonal-mean ΔFLDS and ΔTCWV (supporting information Figure S3). The linear relations hold for each ensemble member as well (supporting information Tables S1 and S2). The spatial maps of ΔSAT, ΔFLDS, and ΔTCWV across the Arctic domain including both DJF and JJA are shown in supporting information Figure S4.

The ensemble-mean and Arctic-averaged DJF vertical profile temperature and humidity changes due to including LW scattering are negligible in the prescribed SST run (Figures 3e and 3f). However, the counterparts from the SOM runs are positive for all ensemble members and well separated from the prescribed SST run results. The change of cloud amount vertical profile, however, is ~1% or even less, and the results from the prescribed SST and SOM runs are not well separated from each other (Figure 3g). These results suggest that the contrast of DJF Arctic ΔSAT between the SOM and prescribed SST runs is not primarily due to a
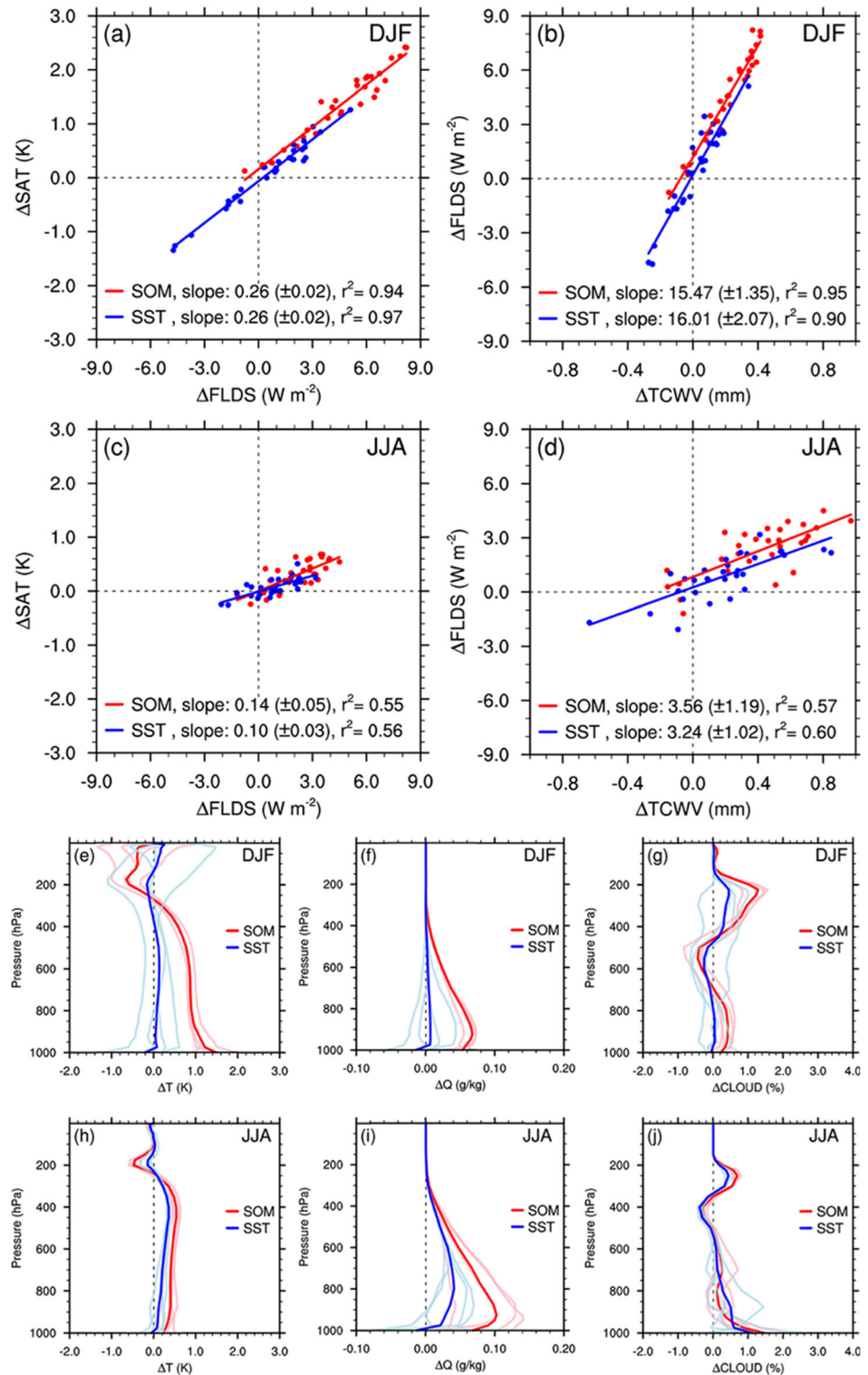
Figure 3. (a) Ensemble-mean, Arctic domain-averaged Scat-noScat difference of SAT (ΔSAT) with respect to the difference of FLDS (ΔFLDS) for each DJF. Results from the SOM and prescribed SST runs are plotted as red and blue dots, respectively. The linear regression lines are also plotted. The numbers in parentheses are 95% confidence intervals. (b) Same as (a) but for ΔFLDS with ΔTCWV. (c, d) Same as (a) and (b), respectively, but for summer (JJA). (e–g) Difference in Arctic domain averaged vertical temperature, humidity, and cloud amount profiles for DJF, ensemble-mean results shown in thick colored lines and results from individual members in thin lightly colored lines. (h–j) Same as (e)–(g) but for JJA.

Table 1
Arctic Domain-Averaged Analysis of the Changes (Δ) Caused by the Inclusion of Ice Cloud LW Scattering

Δ: The difference between Scat and noScat simulations

δ: The difference between SOM and SST simulations

$\Delta FLDS = \beta_1 \Delta TCWV + c_1$; $\Delta SAT = \beta_2 \Delta FLDS + c_2$; $\Delta SAT = \beta_3 \Delta TCWV + c_3$

	Prescribed SST	SOM	δ difference (SOM-prescribed SST)	Estimated difference
β_1	16.0 ± 2.1 (90.0%)	15.5 ± 1.3 (95.2%)		
β_2	0.26 ± 0.02 (97%)	0.26 ± 0.02 (94%)		
β_3	4.02 ± 0.73 (82%)	3.95 ± 0.61 (86%)		
ΔT_{700} (K)	0.11	0.88	0.77	
$\Delta TCWV$ (mm)	0.021	0.22	0.20	
$\Delta FLDS$ (W m^{-2})	0.53	4.56	4.03	$\delta(\Delta FLDS) = \beta_1 \delta(\Delta TCWV)$ 3.2 ± 0.41 3.1 ± 0.26
ΔSAT (K)	0.075	1.35	1.27	$\delta(\Delta SAT) = \beta_1 \beta_2 \delta(\Delta TCWV)$ 0.83 ± 0.06 0.81 ± 0.06 $\delta(\Delta SAT) = \beta_3 \delta(\Delta TCWV)$ 0.80 ± 0.15 0.79 ± 0.12

Note. Linear regression coefficients show 95% confidence intervals and (in parentheses) the fraction of variance explained by the linear regression. In the right column, regression-based differences from the prescribed SST and SOM runs are in blue and red, respectively.

local cloud field change. Instead, it is due to a LW atmosphere-surface feedback mechanism: Including LW scattering leads to an increase of FLDS, which in the wintertime alters the surface energy budget significantly and leads to an increase of surface temperature over the entire Arctic. This surface warming leads to an increase of tropospheric temperature and humidity, which further increases the downward LW flux and forms a positive feedback. This feedback mechanism is particularly effective in the winter as the summer surface temperature can be affected by multiple factors besides FLDS and the summer Arctic ocean SST is largely fixed at the melting point of ice.

To further quantify the contributions of atmosphere-surface LW coupling to the simulated impact of cloud LW scattering, a domain-averaged analysis is performed. The Arctic-averaged DJF ΔTCWV due to ice cloud LW scattering is 0.02 mm in the prescribed SST run but 0.22 mm in the SOM run (Table 1): Surface-atmosphere coupling amplifies the impact of LW cloud scattering on the simulated wintertime TCWV by a factor of 10. A similar drastic contrast between the prescribed SST and SOM runs can be seen for ΔFLDS. Such drastic contrasts are consistent with Figure 3 and confirm the need to consider surface-atmosphere LW coupling to assess the full impact of ice cloud LW scattering in the polar regions.

Since prescribed SST runs do not have surface-atmosphere LW coupling regardless of inclusion of cloud scattering or not, we use the contrast between the prescribed SST and SOM runs to assess the atmosphere-surface LW coupling. Because the change of TCWV is highly correlated with the change of tropospheric temperature, we use ΔTCWV as the *sole* linear predictor to represent the change of clear-sky atmospheric state and estimate ΔFLDS and ΔSAT with linear regression, that is,

$$\Delta FLDS = \beta_1 \ \Delta TCWV + c_1, \tag{2}$$

$$\Delta SAT = \beta_2 \ \Delta FLDS + c_2, \tag{3}$$

$$\Delta SAT = \beta_3 \ \Delta TCWV + c_3. \tag{4}$$

The difference in ΔTCWV between the SOM and prescribed SST runs, denoted as δ (ΔTCWV), reflects the difference due to surface-atmosphere LW radiative coupling, that is, $\delta(\Delta TCWV) = (\Delta TCWV)^{SOM} - (\Delta TCWV)^{SST} = (TCWV_{Scat} - TCWV_{noScat})^{SOM} - (TCWV_{Scat} - TCWV_{noScat})^{SST}$. The difference in ΔFLDS and

ΔSAT due to such coupling can be estimated as $\delta(\Delta FLDS) = \beta_1\delta(\Delta TCWV)$, $\delta(\Delta SAT) = \beta_3\delta(\Delta TCWV)$ or $\delta(\Delta SAT) = \beta_2\beta_1\delta(\Delta TCWV)$. Estimated differences based on respective regressions from the SOM and prescribed SST runs are shown in the right column of Table 1 and are highly consistent with each other. Such linear relations with ΔTCWV can explain 3.2 out of the 4.03 W m^{-2} total difference in ΔFLDS and 0.8 out of the 1.27 K total difference in ΔSAT. This supports our explanation that the clear-sky atmospheric responses resulting from the surface-atmosphere LW coupling account for most of the differences caused by ice cloud LW scattering between the prescribed SST and SOM runs.

So far we have discussed the ice cloud LW scattering effect in the Arctic winter and summer. The same conclusion is also valid in the Antarctic winter and summer (supporting information Figures S5 and S6 and Table S3).

4. Conclusion

The cloud LW scattering effect in climate simulations has recently been investigated (Jin et al., 2019; Wu et al., 2019; Zhao et al., 2018), but all relevant studies have used prescribed SST runs. We find that, without surface-atmosphere radiative coupling, enhanced LW absorption due to cloud LW scattering has a minor impact on the simulated climate, like what have been shown before. When coupling is allowed, its impact on the polar surface climate is amplified through a positive atmosphere-surface feedback, especially in winter, due to the seasonally varying role of LW radiation in determining surface temperature. The domain-averaged budget analysis further quantifies the importance of modeling atmosphere-surface LW coupling to correctly assess the role of cloud LW scattering. These indicate that cloud LW scattering is an indispensable process for high-latitude climate simulation and thus should be included in all climate models, instead of an option. We also show that far-IR scattering dominates the impact of ice cloud LW scattering on the simulated polar surface climate, supporting the need to monitor and understand the role of far-IR radiation on the polar climate (Chen et al., 2014). In a nutshell, our study stresses two overlooked points: (1) coupled simulations are needed to correctly assess the parameterizations of atmospheric processes and (2) a good approximation in some climate zones may not be applicable to other climate zones.

We further compare the change of FLDS due to scattering with the intermodel spread of FLDS in the CMIP6 models. Including ice cloud LW scattering increases the Arctic and Antarctic winter FLDS by 4.6 and 5.2 W m^{-2}, respectively (supporting information Figure S7). The standard deviations of the Arctic and Antarctic winter FLDS simulated by 13 climate models participating in the CMIP6 are 9.8 and 7.9 W m^{-2} respectively (supporting information Table S4). None of these climate models has LW scattering incorporated, and their prescribed SST simulations are used for this analysis. Thus, the difference in FLDS caused by ignoring ice cloud LW scattering is comparable to the intermodel spread of FLDS, implying that the effect of ice cloud LW scattering is not negligible. This further strengthens our argument that cloud LW scattering should be included in climate models.

Data Availability Statement

The standard CESM 1.1.1 package can be downloaded online (http://www.cesm.ucar.edu/models/cesm1.1/index.html). The modified CESM code with LW scattering capability, as well as the code and data used to generate all figures, is available online (https://zenodo.org/record/4274297#.X7Q_nhNKjPY). MERRA-2 data used in the supporting information are downloaded online (https://gmao.gsfc.nasa.gov/reanalysis/MERRA-2/data_access). Spectral flux values used in the supporting information can be downloaded online (https://disc.gsfc.nasa.gov/datasets/AIRSIL3MSOLR_6.1/summary?keywords=AIRSIL3MSOLR_6.1).

References

Baum, B. A., Yang, P., Heymsfield, A. J., Schmitt, C. G., Xie, Y., Bansemer, A., et al. (2011). Improvements in shortwave bulk scattering and absorption models for the remote sensing of ice clouds. *Journal of Applied Meteorology and Climatology*, *50*(5), 1037–1056. https://doi.org/10.1175/2010JAMC2608.1

Chen, X., Huang, X., & Flanner, M. G. (2014). Sensitivity of modeled far-IR radiation budgets in polar continents to treatments of snow surface and ice cloud radiative properties. *Geophysical Research Letters*, *41*, 6530–6537. https://doi.org/10.1002/2014GL061216

Costa, S. M. S., & Shine, K. P. (2006). An estimate of the global impact of multiple scattering by clouds on outgoing long-wave radiation. *Quarterly Journal of the Royal Meteorological Society*, *132*(616), 885–895. https://doi.org/10.1256/qj.05.169

Edwards, J., & Slingo, A. (1996). Studies with a flexible new radiation code. I: Choosing a configuration for a large-scale model. *Quarterly Journal of the Royal Meteorological Society*, *122*(531), 689–719. https://doi.org/10.1256/smsqj.53106

Fu, Q., & Liou, K. N. (1993). Parameterization of the radiative properties of cirrus clouds. *Journal of the Atmospheric Sciences*, *50*(13), 2008–2025. https://doi.org/10.1175/1520-0469(1993)050<2008:POTRPO>2.0.CO;2

Fu, Q., Liou, K. N., Cribb, M. C., Charlock, T. P., & Grossman, A. (1997). Multiple scattering parameterization in thermal infrared radiative transfer. *Journal of the Atmospheric Sciences*, *54*(24), 2799–2812. https://doi.org/10.1175/1520-0469(1997)054<2799:MSPITI>2.0.CO;2

Heymsfield, A. J., Schmitt, C., & Bansemer, A. (2013). Ice cloud particle size distributions and pressure-dependent terminal velocities from in situ observations at temperatures from 0° to −86°C. *Journal of the Atmospheric Sciences*, *70*(12), 4123–4154. https://doi.org/10.1175/JAS-D-12-0124.1

Heymsfield, A. J., Schmitt, C., Bansemer, A., & Twohy, C. H. (2010). Improved representation of ice particle masses based on observations in natural clouds. *Journal of the Atmospheric Sciences*, *67*(10), 3303–3318. https://doi.org/10.1175/2010JAS3507.1

Hurrell, J. W., Holland, M. M., Gent, P. R., Ghan, S., Kay, J. E., Kushner, P. J., et al. (2013). The community earth system model: A framework for collaborative research. *Bulletin of the American Meteorological Society*, *94*(9), 1339–1360. https://doi.org/10.1175/BAMS-D-12-00121.1

Jin, Z., Zhang, Y., Del Genio, A., Schmidt, G., & Kelley, M. (2019). Cloud scattering impact on thermal radiative transfer and global longwave radiation. *Journal of Quantitative Spectroscopy and Radiative Transfer*, *239*, 106669. https://doi.org/10.1016/j.jqsrt.2019.106669

Kristjánsson, J. E., Edwards, J. M., & Mitchell, D. L. (2000). Impact of a new scheme for optical properties of ice crystals on climates of two GCMs. *Journal of Geophysical Research*, *105*(D8), 10,063–10,079. https://doi.org/10.1029/2000JD900015

Kuo, C. P., Yang, P., Huang, X., Chen, Y. H., & Liu, G. (2020). Assessing the accuracy and efficiency of longwave radiative transfer models involving scattering effect with cloud optical property parameterizations. *Journal of Quantitative Spectroscopy and Radiative Transfer*, *240*, 106683. https://doi.org/10.1016/j.jqsrt.2019.106683

Kuo, C.-P., Yang, P., Huang, X., Feldman, D., Flanner, M., Kuo, C., & Mlawer, E. J. (2017). Impact of multiple scattering on longwave radiative transfer involving clouds. *Journal of Advances in Modeling Earth Systems*, *9*, 3082–3098. https://doi.org/10.1002/2017MS001117

McClatchey, R. A., Fenn, R. W., Selby, J. E. A., Volz, F. E., & Garing, J. S. (1972). Optical properties of the atmosphere, Air Force Cambridge research labs, Environmental research paper, No. 411.

Mitchell, D. L., Liu, Y., & Macke, A. (1996). Modeling cirrus clouds. Part II: Treatment of radiative properties. *Journal of the Atmospheric Sciences*, *53*(20), 2967–2988. https://doi.org/10.1175/1520-0469(1996)053<2967:MCCPIT>2.0.CO;2

Mlawer, E. J., Taubman, S. J., Brown, P. D., Iacono, M. J., & Clough, S. A. (1997). Radiative transfer for inhomogeneous atmospheres: RRTM, a validated correlated-k model for the longwave. *Journal of Geophysical Research*, *102*(D14), 16,663–16,682. https://doi.org/10.1029/97JD00237

Neale, R. B., Richter, J. H., Conley, A. J., Park, S., Lauritzen, P. H., Gettelman, A., et al. (2010). Description of the NCAR community atmosphere model (CAM 4.0). NCAR technical note, *NCAR/TN-485+STR*.

Neale, R. B., Chen, C.-C., Gettelman, A., Lauritzen, P. H., Park, S., Williamson, D. L., et al. (2012). Description of the NCAR community atmosphere model (CAM 5.0). NCAR technical note, *NCAR/TN-486+STR*.

Overland, J. E., & Guest, P. S. (1991). The Arctic snow and air temperature budget over sea ice during winter. *Journal of Geophysical Research*, *96*(C3), 4651. https://doi.org/10.1029/90JC02264

Pincus, R., Barker, H. W., & Morcrette, J.-J. (2003). A fast, flexible, approximate technique for computing radiative transfer in inhomogeneous cloud fields. *Journal of Geophysical Research*, *108*(D13), 4376. https://doi.org/10.1029/2002JD003322

Platnick, S., Meyer, K. G., King, M. D., Wind, G., Amarasinghe, N., Marchant, B., et al. (2017). The MODIS cloud optical and microphysical products: Collection 6 updates and examples from Terra and Aqua. *IEEE Transactions on Geoscience and Remote Sensing*, *55*(1), 502–525. https://doi.org/10.1109/TGRS.2016.2610522

Randall, D. A. (1989). Cloud parameterization for climate modeling: Status and prospects. *Atmospheric Research*, *23*(3–4), 345–361. https://doi.org/10.1016/0169-8095(89)90025-2

Serreze, M. C., & Barry, R. G. (2005). *The Arctic climate system* (p. 385). Cambridge: Cambridge University Press. https://doi.org/10.1017/CBO9780511535888

Stamnes, K., Tsay, S.-C., Wiscombe, W., & Jayaweera, K. (1988). Numerically stable algorithm for discrete-ordinate-method radiative transfer in multiple scattering and emitting layered media. *Applied Optics*, *27*(12), 2502. https://doi.org/10.1364/AO.27.002502

Stephens, G. L. (1984). The parameterization of radiation for numerical weather prediction and climate models. *Monthly Weather Review*, *112*(4), 826–867. https://doi.org/10.1175/1520-0493(1984)112<0826:TPORFN>2.0.CO;2

Stephens, G. L. (2005). Cloud feedbacks in the climate system: A critical review. *Journal of Climate*, *18*(2), 237–273. https://doi.org/10.1175/JCLI-3243.1

Toon, O. B., McKay, C. P., Ackerman, T. P., & Santhanam, K. (1989). Rapid calculation of radiative heating rates and photodissociation rates in inhomogeneous multiple scattering atmospheres. *Journal of Geophysical Research*, *94*(D13), 16,287–16,301. https://doi.org/10.1029/JD094iD13p16287

Wu, K., Li, J., Cole, J., Huang, X., von Salzen, K., & Zhang, F. (2019). Accounting for several infrared radiation processes in climate models. *Journal of Climate*, *32*(15), 4601–4620. https://doi.org/10.1175/JCLI-D-18-0648.1

Yang, P., Liou, K.-N., Bi, L., Liu, C., Yi, B., & Baum, B. A. (2015). On the radiative properties of ice clouds: Light scattering, remote sensing, and radiation parameterization. *Advances in Atmospheric Sciences*, *32*(1), 32–63. https://doi.org/10.1007/s00376-014-0011-z

Zhao, W., Peng, Y., Wang, B., & Li, J. (2018). Cloud longwave scattering effect and its impact on climate simulation. *Atmosphere*, *9*(4), 153. https://doi.org/10.3390/atmos9040153

References From the Supporting Information

Huang, X., Chen, X., Potter, G. L., Oreopoulos, L., Cole, J. N. S., Lee, D., & Loeb, N. G. (2014). A global climatology of outgoing longwave spectral cloud radiative effect and associated effective cloud properties. *Journal of Climate*, *27*(19), 7475–7492. https://doi.org/10.1175/JCLI-D-13-00663.1

Kay, J. E., Bourdages, L., Miller, N. B., Morrison, A., Yettella, V., Chepfer, H., & Eaton, B. (2016). Evaluating and improving cloud phase in the Community Atmosphere Model version 5 using spaceborne lidar observations. *Journal of Geophysical Research: Atmospheres*, *121*, 4162–4176. https://doi.org/10.1002/2015JD024699

Kay, J. E., Deser, C., Phillips, A., Mai, A., Hannay, C., Strand, G., et al. (2015). The community earth system model (CESM) large ensemble project: A community resource for studying climate change in the presence of internal climate variability. *Bulletin of the American Meteorological Society*, *96*(8), 1333–1349. https://doi.org/10.1175/BAMS-D-13-00255.1

Morrison, A. L., Kay, J. E., Frey, W. R., Chepfer, H., & Guzman, R. (2019). Cloud response to Arctic sea ice loss and implications for future feedback in the CESM1 climate model. *Journal of Geophysical Research: Atmospheres*, *124*, 1003–1020. https://doi.org/10.1029/2018JD029142